Dynamical analysis of the ν Octantis planetary system

K. Goździewski, M. Słonina, A. Rozenkiewicz & C. Migaszewski

Toruń Centre for Astronomy, k.gozdziewski@astri.umk.pl

Introduction

The ν Oct is a single–line spectroscopic binary composed of ν Oct A, K1 III giant primary (1.4 ± 0.3 M$_\odot$), and unseen red dwarf secondary ν Oct B, K7-M1 V (0.5 ± 0.1 M$_\odot$) separated by $\sim 2.55 \pm 0.13$ au. Already in 1935, Colacevich [5] collected 11 radial velocities (RVs) of the primary, and Alden [2] determined Keplerian elements of the astrometric orbit. Remarkably, the inclination $i_{\mathrm{bin}} = 71°$ is recently known with an error of less than $1°$ on the basis of Hipparcos astrometry and 223 precision RVs collected by Ramm et al. [13]. Yet these authors discovered residual variability of the RVs that has been attributed to a Jovian planet of mass $m_{\mathrm{p}} \sin i_{\mathrm{p}} = 2.5$ M$_{\mathrm{Jup}}$.

The announced planet is quite unusual, because the derived semi-major axis $a_{\mathrm{p}} \sim 1.2 \pm 0.1$ au implies it orbits in the middle between the massive primary and secondary. Besides the formation of this planet in the binary can be hardly explained, any analytic or general stability criteria in the three-body problem or in the restricted three-body problem, including criteria by the Hill, Holman & Wiegert [10], the resonance-overlap criterion by Wisdom [14] and other (see [12]), are violated. Indeed, Eberle & Cunz [6] found the proposed Keplerian solution strongly unstable in just 1–10 binary periods time-scale. That contradicts the planetary hypothesis, although the discovery paper excludes non-planetary sources of the observed signal, like stellar spots or pulsations.

There could be alternate explanations of the observed RVs variability. An interesting and original model has been proposed at this conference, which regards the orbital configuration of a hierarchical triple system with an unseen binary at the place of the secondary ν Oct B. That would force a precession of the primary orbit around the barycentre of that inner binary and it could mimic a signal attributed to the identified putative planet [11]. Other causes of the residual RVs can be an unmodeled stellar variability, a different number of planetary companions, systematic errors of the observations, including instrumental instabilities and non-Gaussian uncertainties, e.g., the red noise [3], or a quite different orbital model (see below).

Indeed, [6] found that a *retrograde* orbit of the planet lies in a stable zone much wider than in the direct configuration. However, the analysis of the RVs done in both cited papers does not seem consistent with the dynamical character of the system. The mass of the secondary might be almost half of the primary mass, hence the relatively wide planetary is strongly *perturbed*. In the ν Oct, the perturbation parameter (mass ratio of the secondary and the primary) might be as large as 0.3–0.5. Furthermore, it has been assumed that the whole system is co-planar, no matter the planetary orbit is prograde or retrograde. However, non-planar orbits in compact binaries may likely appear due to violent post–formation scenarios, like planet–planet scattering [1] that may lead to highly inclined configurations. Finally, the dynamical simulations done in [6] concern very particular initially aligned orbits, that maximises the chance of stable configurations but does not necessarily reproduce the reflex motion of the primary. Because the phase space of strongly interacting system is non-continuous in terms of stability, the relative orbital phases should not be fixed *a priori*, if supposed to be consistent with observations.

In this paper, we try to verify and improve the kinematic (Keplerian) model of the ν Oct planetary system by searching for the best-fit configurations in terms of self-consistent dynamical, *N*-body model, along e.g. [8] and references therein. To resolve the fine structure of the phase space of strongly perturbed dynamical system, we apply the fast-indicator MEGNO [4] code adapted to our new multi-CPU computing environment MECHANIC (see our second paper in this volume). More details and technical aspects of our work will be described and published elsewhere [15].
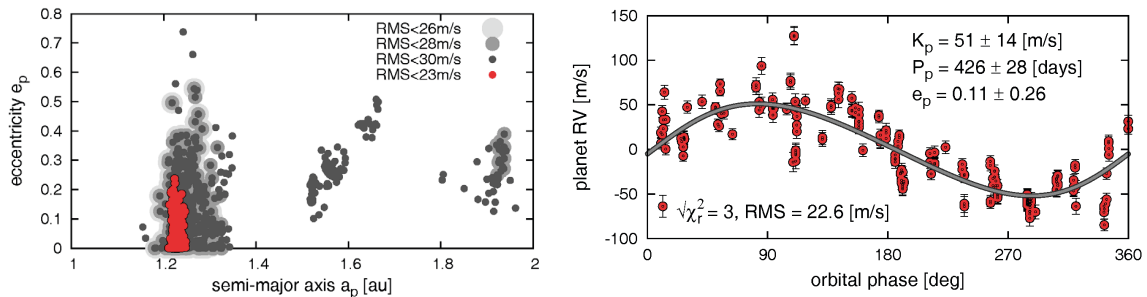
Figure 1: *The left-hand panel*: statistics of Keplerian best-fit models projected onto the semi-major axis — eccentricity (a_p, e_p)-plane gathered in the hybrid search. Best-fit configurations with an RMS$<$ 23ms^{-1} are marked with filled red circles. *The right-hand panel*: synthetic curve of the best fit model over-plotted with the planetary residual signal, after subtracting the RVs due to the secondary. The Keplerian elements are labeled on the plot.

1. Keplerian model and the system stability

To verify the results in [13], we performed a hybrid search for the Keplerian orbits of the putative planet, which relies on the Genetic Algorithms and a fast local optimization scheme [8]. We used only the RV measurements in [13]. Their formal errors have been rescaled by a stellar jitter of ~ 5 ms^{-1} in quadrature. The results are shown in Fig. 1. The left-hand panel illustrates the best-fit parameters projected onto the semi–major axis–eccentricity plane. Configurations providing smallest RMS< 22 ms^{-1} are marked with red filled dots, and gradually "worse" solutions with larger, shaded circles that are labelled. We can confirm that the best-fit, moderate-eccentricity Keplerian orbit is found close to ~ 1.2 au, and it corresponds to a strongly unstable configuration. We found two other, although worse solutions families around ~ 1.6 au and 2 au, respectively. These fits cannot be skipped *a priori* because the RV signal of putative planet (the right-hand panel in Fig. 1) is very noisy, and the residuals have an amplitude similar to the signal itself, in the light of reported formal measurements errors at the level of 5 ms^{-1}. That may put the discovery in doubt, nevertheless we decided to test the planetary hypothesis on the dynamical grounds.

For that we performed extensive numerical mappings of the phase space, following the hypothesis of [6]. They searched for stable orbits at discrete grid of primary mass $(1.1, 1.4$ and $1.7)$ M$_\odot$, three mass ratios $(\mu = 0.2593, 0.2754, 0.2908)$, and 30–step initial distance ratio ρ between the planet and the secondary, $\rho \in \langle 0.22, 0.54 \rangle \equiv \langle 0.56, 1.38 \rangle$ au. The *N*-body equations of motion have been integrated over 10^3 years $(\sim 350$ binary periods $P_{bin})$ for prograde orbits, and over 10^4 years $(\sim 3500\ P_{bin})$ for retrograde orbits. The initial orbits have been *aligned*, and both secondaries fixed in their apoastrons with respect to the primary. These integrations confirm the theoretical stability limit $\rho \sim 0.25 \equiv 0.64$ au for prograde orbits. For the retrograde case, the stability limit has been found much larger, indeed, $\rho \sim 0.479$ (1.22 au), claimed in agreement with the formal error [13]. However, in configuration stable over 10 Myr [6], $a_p \sim \rho_0 \times a_{bin}/(1 + e_p) \simeq 0.86$ au, where $\rho_0 = 0.379$, $a_{bin} \sim 2.55$ au), and $e_p = 0.123$, hence the osculating semi-major axis a_p has been fixed relatively different from the formal solution.

We fixed all angles and planetary elements as in [6], the mass of the primary to 1.4 M$_\odot$, $\mu = 0.28$ (i.e., as
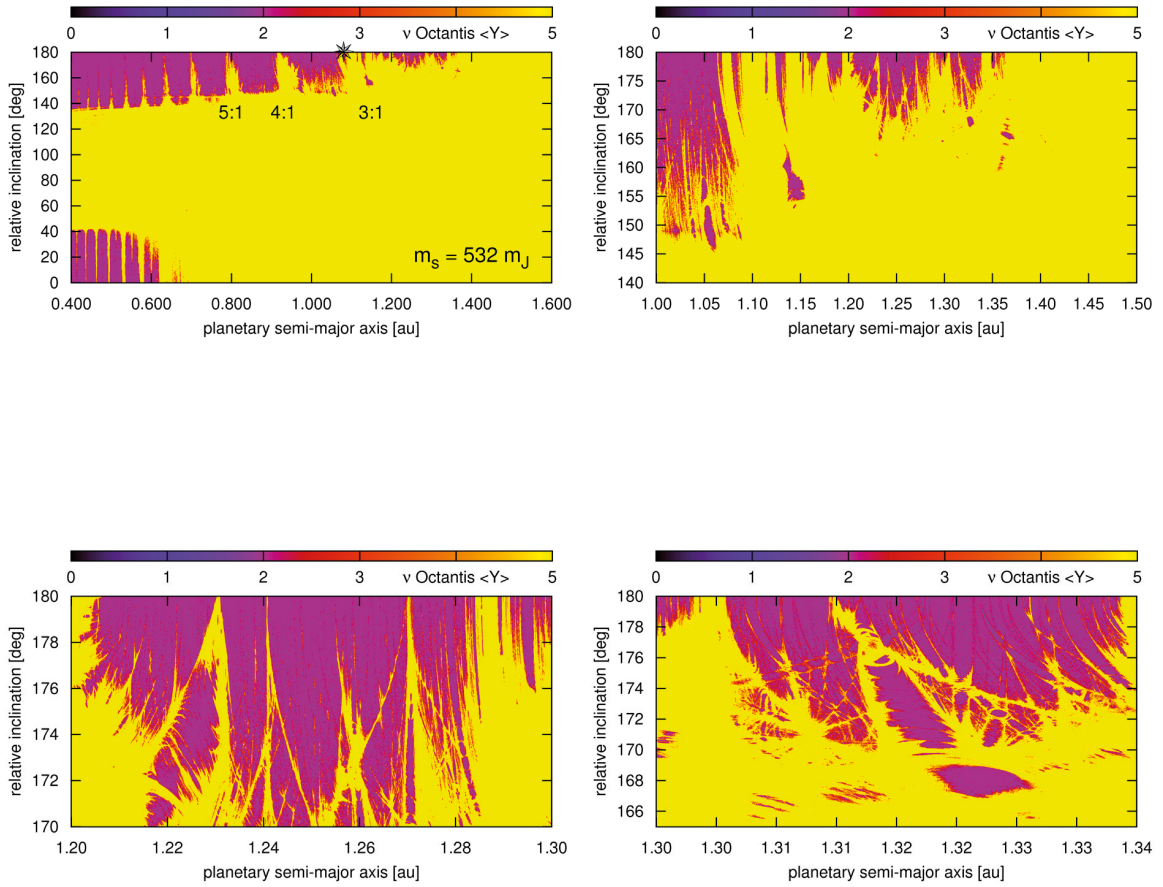
Figure 2: Dynamical maps for the initial condition examined by Eberle & Cuntz [6] in the planetary semi-major axis – relative inclination ($a_\mathrm{p}, i_\mathrm{rel}$)-plane. Masses and parameters of the binary are fixed at their values in [6]. Initial orbits are aligned, with the secondary and the planet fixed at apoastrons. Stability is colour-coded: yellow means strongly unstable motions, and dark magenta is for quasi-periodic solutions (MEGNO $Y \sim 2$).

in their Fig. 2), and then we computed high-resolution (1440×900 pixels) MEGNO maps over 25,000 periods of the binary. The results are shown in Fig. 2 at the semi–major a_p — relative inclination i_{rel} plane. The top left-hand panel illustrates the phase space globally, and three subsequent maps are for close-ups of a region, in which the planet might be present. That experiment confirms the stability limit almost two times farther for retrograde than prograde orbits. The phase space is filled with unstable MMRs. Overlapping of these resonances and their sub-resonances creates global chaotic zone beyond ~ 0.6 au for prograde orbits, and ~ 1.0 au for retrograde orbits, that is supposed the main source of instability in binaries [12]. Configurations with intermediate relative inclinations are very chaotic, particularly close to polar orbits ($i_{rel} \sim 90°$), and most likely are associated with the Kozai resonance. A stable retrograde orbit found in [6] lies in a region spanned by strong 4:1, 3:1, 5:2 and 2:1 MMRs. Moreover, close-ups of this area reveal a complex net of stable and unstable motions that might be identified with the so called Arnold web found in perturbed, low-dimensional Hamiltonian systems, and in the Outer Solar system [7, 4, 9]. Yet it is now clear that finding stable orbit at a sparse, equidistant grid could be done basically only by chance.

2. Self-consistent Newtonian model with stability constraints

To improve the Keplerian model, we conducted a search for stable models in terms of the *N*-body problem imposing a stability constraint (GAMP algorithm, [8]). We fixed a binary inclination $i_{bin} = 71°$ and its nodal line $\Omega_{bin} = 87°$ [13]. Masses of secondaries, planet inclination i_p, its nodal longitude Ω_p and remaining elements were fitted. The results are shown in Fig. 3. Quality of the fits is expressed by an RMS, and labeled in panels. Filled, red circles mark regular fits, that have MEGNO signature ~ 2 over 2000 P_{bin}, providing at least 10-100 times longer stability time.

An inspection of the gathered statistics reveals that the planetary orbit is not well constrained by the *N*-body model (blue filled circles). Stable solutions (red filled circles, with RMS$< 25 \text{ms}^{-1}$) are found *only* for retrograde orbits, in agreement with the Eberle & Cuntz hypothesis, nevertheless initially almost exactly *anti–aligned* with the binary orbit, contrary to their *aligned* orbital setup. Besides, we found the best–fit configurations with RMS~ 20 ms^{-1} for $a_p \sim 1.6$ au, that would correspond to one of minima identified in Fig. 1. Yet these fits are very unstable.

The left-hand panel of Fig. 4 illustrates the MEGNO dynamical map in the (a_p, i_p)–plane for the global view of the phase space (the left-hand panel), which is mostly strongly chaotic. A close-up (the right-hand panel) reveals relatively very small regular island of the best-fit stable model found in the GAMP search (see its elements in caption to Fig. 4). In that island, the phase space has again a very complex structure of the Arnold web.

Conclusion

We confirmed a hypothesis of stable retrograde orbit in [6]. However, the observational constrains require such orbits initially *anti-aligned* with the binary orbit. Besides, stable models may be found only in a small island with complex Arnold web structure. Although the best-fit is rigorously stable, it remains uncertain how the planet could be trapped in such a small stable region, or how it could be formed in globally unstable dynamical environment. Besides, the RV signal is very noisy, and the best-fit models reveal a large scatter of residuals having amplitude comparable with the RV signal itself. A presence of Jovian planet in orbit around ν Oct A is questionable, and new observations are required to confirm or withdraw that explanation of the observed RV residual signal.
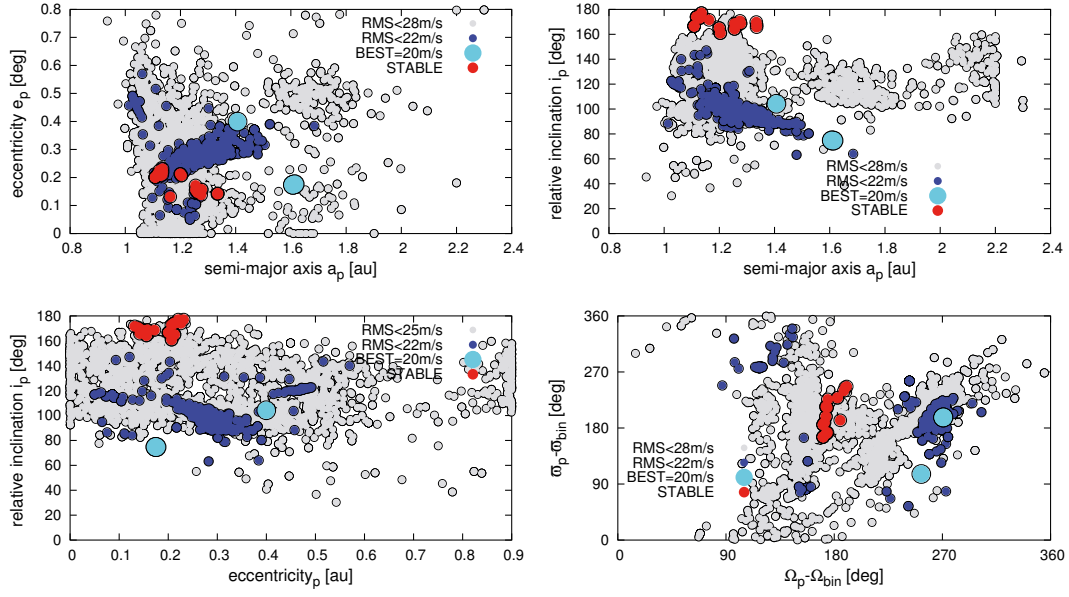
Figure 3: Statistics of the *N*-body and GAMP best-fit models projected onto planes of orbital osculating elements at the epoch of the first observation in [13], gathered in the hybrid search. A RMS quality of these solutions is marked with filled circles and labeled in the plots. Configurations found with imposed stability constraints, and detected as stable by the GAMP algorithm, are marked with filled red circles.
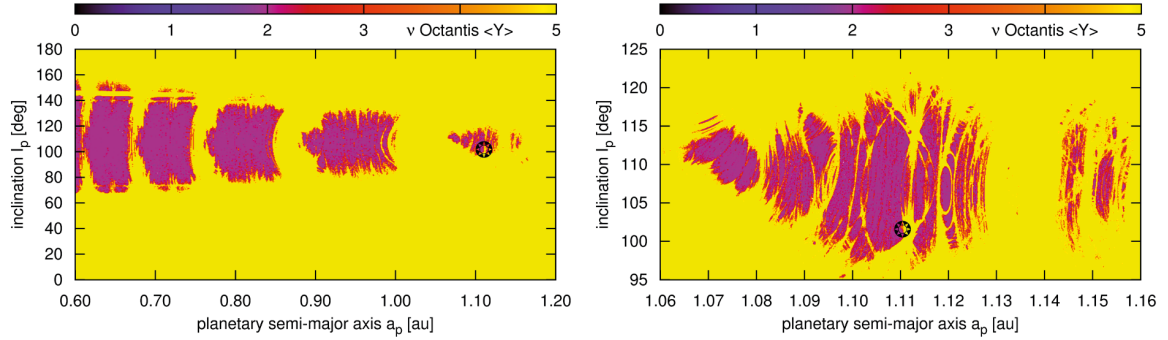
Figure 4: MEGNO maps of stable best–fits found in the GAMP search (note *the absolute* inclination). Nominal elements are marked with the star. Osculating, *astrocentric* elements of the planet at the first epoch in [13] are $m_p = 1.92596\,M_{Jup}$, $a_p = 1.16365$, $e_p = 0.13139$, $i_p = 110.21102°$, $\Omega_p = 262.29811°$, $\omega_p = 127.26299°$, mean anomaly $M_p = 133.16327°$, respectively. Elements of the secondary are $m_s = 560.62366\,M_{Jup}$, $a_{bin} = 2.52813$, $e_{bin} = 0.23881$, $i_{bin} = 71.28090°$, $\Omega_{bin} = 87.0°$, $\omega_{bin} = 74.59137°$, $M_s = 339.762973°$, respectively. We quoted many digits, to reproduce the fit possibly exactly, due to complex and chaotic neighborhood. Its formal error may be estimated graphically in Fig. 3. Mass of the primary is fixed at $1.4\,M_\odot$. The RMS of this solution is $\sim 25\,\mathrm{ms}^{-1}$.

References

[1] Adams F. C. and Laughlin G. 2003. *Icarus*, 163, 290–306.

[2] Alden H. L. 1939. *AJ*, 48, 81–84.

[3] Baluev R. V. 2011. *Celestial Mechanics and Dynamical Astronomy*, 111, 235–266.

[4] Cincotta P. M., Giordano C. M., and Simó C. 2003. *Phys. D*, 182, 151–178.

[5] Colacevich A. 1935. *PASP*, 47, 87.

[6] Eberle J. and Cuntz M. 2010. *ApJL*, 721, L168–L171.

[7] Froeschlé C., Guzzo M., and Lega E. 2000. *Science*, 289, 2108–2110.

[8] Goździewski K., Migaszewski C., and Musieliński A. 2008. *IAU Symposium 249*, 249, 447–460.

[9] Guzzo M. 2005. *Icarus*, 174, 273–284.

[10] Holman M. J. and Wiegert P. A. 1999. *AJ*, 117, 621–628.

[11] Morais M. H. M. and Correia A. C. M. 2011. *MNRAS*.

[12] Mudryk L. R. and Wu Y. 2006. *ApJ*, 639, 423–431.

[13] Ramm D. J., Pourbaix D., Hearnshaw J. B., and Komonjinda S. 2009. *MNRAS*, 394, 1695–1710.

[14] Wisdom J. 1980. *AJ*, 85, 1122–1133.

[15] Slonina et al. 2012, in preparation.